

## Article

# Analytical Approach Based on Full-Space Synergy Technology to Optimization Support Design of Deep Mining Roadway

Shike Zhang <sup>1,\*</sup> and Shunde Yin <sup>2</sup><sup>1</sup> School of Civil Engineering and Architecture, Anyang Normal University, Anyang 455000, China<sup>2</sup> Department of Civil and Environmental Engineering, University of Waterloo, Waterloo, ON N2L 3G1, Canada; s2yin@uwaterloo.ca

\* Correspondence: shikezhang@aynu.edu.cn; Tel.: +86-182-7256-9128

**Abstract:** The stability of surrounding rock is the basic guarantee of underground space engineering safety. The large deformation of a roadway's surrounding rock is a very common phenomenon during the underground excavation of coal mine roadways or coal mining, especially in deep soft rock mining roadways. With the increase in mining depth and mining stress, it is very important to prevent disasters caused by surrounding rock deformation. This work aims to conduct an optimization design of roadway support for deep soft rock in coal mines using a full-space synergy control technology. FLAC3D-based orthogonal numerical experiments are adopted to study the influence of bolt parameters and plastic yield zone variation on the deformation of roadway surrounding rock, which provides a basis for optimizing the support design of coal mine roadways. According to the results of the numerical analysis, the optimal support parameters are determined as 20 mm, 2.2 m and 700–900 mm for diameter, length and interval of the bolt, respectively. Finally, the determined bolt-shotcrete net beam support scheme from the full-space synergy control idea is used in a study case. Results illustrate that this study can provide reliable guidance for the stability control of deep soft rock roadways in mining fields under high stress, and it can work well to keep the surrounding rock deformation within the safe limits.

**Keywords:** full-space synergy method; bolt support optimization design; orthogonal experiment; numerical analytical approach; deep soft roadway



**Citation:** Zhang, S.; Yin, S. Analytical Approach Based on Full-Space Synergy Technology to Optimization Support Design of Deep Mining Roadway. *Minerals* **2022**, *12*, 746. <https://doi.org/10.3390/min12060746>

Academic Editors: Afshin Asadi and Mamadou Fall

Received: 2 April 2022

Accepted: 10 June 2022

Published: 12 June 2022

**Publisher's Note:** MDPI stays neutral with regard to jurisdictional claims in published maps and institutional affiliations.



**Copyright:** © 2022 by the authors. Licensee MDPI, Basel, Switzerland. This article is an open access article distributed under the terms and conditions of the Creative Commons Attribution (CC BY) license (<https://creativecommons.org/licenses/by/4.0/>).

## 1. Introduction

Coal is one of the most important mineral resources in China. Due to the rapid development of China's economy, large quantities of coal resources in shallow mining have been basically depleted, so the mining of most coal resources has moved to the deep-lying stratum [1–3]. With the increase in the mining depth, both the frequency and intensity of the coal mining engineering risk in the underground stope are increasing, such as rock burst, soft rock large deformation, water inrush and flowing deformation [4–6], which brings tremendous threat to the efficient mining of coal resources and the safety of miners. For the deep soft rock mining roadway, the structural instability and nonlinear large deformation of surrounding rock are the most common problems with the stress environment's deterioration [7]. In practice, roof fall, rib spalling and floor heave exist to different degrees in massive cases, and these problems are also very difficult to address [8,9]. If this kind of unstable surrounding rock support problem can be effectively addressed, there is great significance to the safe production of coal mines. Because large deformation or flowing deformation of the surrounding rock can lead to the failure of the roadway and the working environment becomes unsafe, coal mining is not able to continue. Thus, numerous investigations on the stability control technology and support schemes of the surrounding rock of coal mine roadways were performed by researchers and engineers, and lots of beneficial correction theories and technologies were also proposed by them,

such as full-stress anchoring technology and bolt support [10–14]. However, relatively few studies on hybrid full-space synergy technology and the application of bolts based on the orthogonal experimental method have been launched for the roadway optimization design of mining fields in deep soft rock.

Deep soft rock roadway support is one of the focus issues in deep mining engineering due to the complicacy and particularity of mining conditions [15–18]. The geological features of the deep roadway surrounding rock of a coal mine are usually summed up as “three highs and one disturbance”: high geo-stress, high earth temperature, high karst water pressure and strong mining disturbance [19]. Researchers and engineers have carried out numerous studies on mechanical mechanisms and support technology for deep roadways and have obtained some achievements in terms of the indoor experiment, field test, theoretical analysis and numerical simulation.

In practical engineering, the laboratory and/or field test of rock masses are often necessary because they can efficiently estimate the failure mechanisms of surrounding rock and provide some basic physical and mechanical parameters of the surrounding rock during the underground engineering design. Wang and Tan [20] applied the indoor experiment to analyze each drill hole core lithology and provide physical and mechanical properties of the soft rock roadway in Yangcheng coal. By a feat of CT technology, Cheon et al. [21] analyzed the failure mechanism and area of surrounding rock based on the physical model experiment under polyaxial stress conditions. Sun et al. [22] used the field test to investigate the deformation mechanism of strong floor heave on deep soft rock roadway and its control technique and believed that the tending time of the stability for roadway surrounding rock after treatment was closely related to the deformation severity of the floor heave. Si et al. [23] studied the effect of loading rate on the rockburst by the true-triaxial test for 100 mm × 100 mm × 100 mm cubic specimens; the results showed that the rockburst of the side surrounding rock was more serious with a decrease in the loading rate. Zhao et al. [24] adopted the pull-out test on the sinistrality rebar bolt specimens with a bolt rib spacing of 12, 24, 36 and 48 mm to study the effect of bolt rib spacing on the anchorage performance with different surrounding rock environments and found that the pulling force of the anchor rod was the highest at a rib spacing of 24 mm. Yu et al. [25] studied the mechanical properties and failure mechanisms of coal-rock-bolt composite surrounding rock mass, and a series of uniaxial compression tests were conducted for the respective non-anchored, and horizontal bolt-anchored coal-rock composited samples with the respective combined angles of 15°, 30° and 45° between the coal and the rock. Jing et al. [26] independently developed a test system for the whole process of deep roadway surrounding rock structure instability to experimentally study the whole failure process of the anchorage structure of a deep roadway. Li et al. [27] investigated the damage and failure characteristics of rock-like material under high in situ stress and dynamic loading using the true triaxial test and the acoustic emission signal technology.

Due to the complexity of the engineering environment of deep roadway surrounding rock, plus limitations of test conditions, the mechanical parameters and failure characteristics of rock mass determined by the test method cannot be completely accurate; investigation of the stability control and failure mechanism of deep soft rock roadway still needs the support and cooperation from theoretical analysis, numerical simulation and intelligent algorithms and others. Wu et al. [28] utilized the numerical orthogonal test and regression analysis method to determine the mechanical properties of the rock mass and combined it with elastic modulus, cohesion, internal friction angle and tensile strength in the laboratory to carry out the optimization design of the stability control of deep soft rock roadways. In [29], the nonlinear large deformation of the surrounding rock in a deep soft rock roadway (e.g., phenomena, characteristics and reasons) was worked out by combining the test method and numerical simulation, and a suitable coupling support countermeasure was put forward for Xin’an Coal Mine in Gansu province, China. Many European countries, such as France, UK, Germany and Poland, conducted research on the theories and techniques of surrounding rock stability control of a deep coal roadway

based on the local geological conditions. In the matter of roadway support technology, the hybrid yieldable steel arches and rock bolt and backfilling beside the roadways and behind the steel arches, are well investigated and used widely [30–32]. The self-excited acoustical system (SAS) was used by Skrzypkowski et al. [33,34] to monitor the stress distribution of the rock strata, and they suggested substituting full-length anchorage rock bolt support for segmented bolt support to control roof deformation in deep mining roadways. Zhao et al. [35] adopted numerical modeling to analyze the technical parameters of the surrounding rock control in a deep coal mine roadway, and the full-section layer double arch synergy reinforcement technology was proposed in practical engineering based on an engineering analogy. Finally, the field monitoring test was used to verify the effectiveness of the optimization support scheme. Malkowski [36] used the finite element method to analyze the stability control problem of the mine roadway; on the basis of the comparison with field monitoring results, Malkowski believed that the choice of the physical model and failure criterion had a distinct influence on the size of the computed failure area of the working surface. In references [37,38], the mechanical behavior of the surrounding rock under different bolt numbers and anchoring parameters was studied by employing the FLAC3D (Fast Lagrangian Analysis of Continua in 3 Dimensions) numerical program from ITASCA (Itasca International Inc., Minnesota, USA), the results illustrated that the bolt anchorage could effectively change the peak strength and elastic modulus of the stratum to accomplish the stability control of surrounding rock in a deep roadway. Tang et al. [39] applied the Universal Discrete Element Code (UDEC) numerical method to study the mechanical mechanism and support design of fractured rock mass roadway when conducting the TBM-excavated roadways of a coal mine. Zuo et al. [40] summarized the mechanical mechanism and failure characteristics of deep roadway surrounding rock and put forward the full-space cooperative control mechanics principle for deep roadways.

As can be seen from the above insufficiently comprehensive literature review, the bolt-anchor coupling support scheme is extensively used in deep soft rock roadways of coal mines, and FLAC3D numerical modeling software is the most widely used because it can simulate the large deformation of soil and rock mass well [41]. In addition, as an active support technology, bolt support can be employed in the advancing support of roadway surrounding rock, and there are relatively high support strength and low support cost. The above research results can basically make it clear that the impact factors of deep roadway deformation mechanisms have the characteristics of diversity, regionalization, time efficiency and anisotropy, plus roadway support schemes have more. Consequently, there is still some room for enhancement in terms of pertinence and effectiveness control for a specific case study of coal mine roadway support by selecting the appropriate mechanical mechanism analysis method and roadway optimization support scheme and parameters.

The goal of this article is to conduct research on the support scheme and parameter optimization on deep soft rock roadways of coal mines, which aims to improve the stability of surrounding rock roadways with nonlinear large deformation and ensure safety in coal mines. In this paper, the stability of the complex underground roadway system of Shishan Coal Mine in Shanxi Province is regarded as the research object, full-space synergy technology is used to optimize the support method and parameters of the deep roadway under different geological conditions, and FLAC3D-based orthogonal numerical experiments are used to perform the sensitivity analysis of bolt parameters for the stability control of the roadway surrounding rock, which is applied in practical engineering. The results of roadway deformation illustrate that the proposed support design scheme is feasible and can effectively control the deformation of the surrounding rock in deep rock roadways.

## 2. Engineering Background

### 2.1. Local Geological Features

The Shishan Coal Mine is located in Shanxi province; the geographic coordinates are almost at 112°32' east longitude and 35°33' northern latitude. It belongs to the Qinshui coalfield, which is a large carboniferous Triassic coalfield; most of the production is based

on anthracite, chemical coal and cooking coal in China. Shishan Coal Mine mainly produces anthracite with a low sulfur content; No. 3, 9, 15 seams are excavating coal resources at present. Thereinto, the average buried depth of the No. 3 coal seam is about 473 m, and the design production capacity is 900 kilotons per year. For the deep No. 3 coal seam, there is a single mine hydrogeological condition and no obvious water inrush at the 3010 working face because the water level is far from the mining seam. In addition, rock burst has no obvious impact on the coal mine safety production because the roadway surrounding rock is in the soft rock stratum.

The No. 3 coal seam of the Shishan Coal Mine is supported by the occurrence stability of the coal seam; the inclination is from 3 to 5 degrees, and its overburden is composed of sandstone, mudstone, siltstone, limestone, subsandy soil, light red subclay and brecciated rock from coal seam to round surface in turn. In numerical modeling, the strata near the coal seam are mainly studied, and a comprehensive histogram of the No. 3 coal seam and rock strata is shown in Figure 1. The thickness of the coal seam is 2.6–5.2 m; the average thickness is about 4.36 m, and its protodyakonov coefficient  $f$  is about 1. There is an immediate roof of mudstone with an average thickness of about 2.1 m; the average protodyakonov coefficient  $f$  is about 2. The main roof is mostly composed of sandy mudstone and fine sandstone with an average thickness of about 5.35 m and 1.01 m, respectively. Above the main roof is mainly composed of muddy siltstone, clayey sandstone and mudstone, and their protodyakonov coefficients  $f$  are mostly distributed between 2 and 6. The lithology of the floor is mainly sandy mudstone and fine sandstone with averages of about 1.03 and 1.86 m, respectively, and their protodyakonov coefficients  $f$  are mostly distributed between 2 and 4. Further down the floor is the medium sandstone with an average of about 5.01 m.

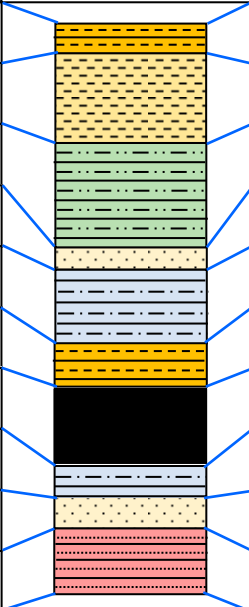
No.	Stratum thickness (m)	Geological column of lithology	Lithologic character	Protodyakonov coefficient $f$
6	1.6		Mudstone	5
5	8.1		Clayey sandstone	4
4	8.47		Muddy siltstone	4
3	1.01		Fine sandstone	2
2	5.35		Sandy mudstone	3
1	2.1		Mudstone	2
0	4.36		No. 3 coal seam	1
-1	1.03		Sandy mudstone	2
-2	1.86		Fine sandstone	3
-3	5.01	Medium sandstone	4	

Figure 1. The comprehensive histogram of No. 3 coal seam and rock strata.

2.2. Deformation and Failure Situation Analysis of Existing Roadway

The original support pattern is an H-shape steel beam, and U29-type steel flexible support in the stope of the No. 3 coal seam, and the top, bottom and height of the trapezoid roadway section are 2.4, 3.6 and 2.1 m, respectively. With the development of the mining depth, the roadway surrounding pressure gradually increases, and the difficulty of support also increases, so that the original support mode cannot meet the requirement at all. Figure 2 is the diagram of the roadway roof fall and flow floor heave with rock squeezing;

the detailed theoretical analysis will be introduced in the next section. The roof has fallen as far as 220 mm, the displacement of two sides can reach 240 mm, and the floor heave is 197 mm at maximum. It started to yield steel beam bending, crack, shed and column bending, roof collapse, etc. The mining roadway has completely collapsed and has become inaccessible in some areas.



**Figure 2.** The roadway roof fall and flow floor heave with rock squeezing.

In the recent excavation, due to the influence of high earth stress, the surrounding rock of the mining roadway yields a large deformation and failure phenomenon. The displacement of the roof, side and floor can reach 40, 45 and 38 mm, respectively. If the deformation cannot be immediately controlled, it will happen via roof fall and wall caving. This has seriously affected the normal production and safety of the mine.

### 2.3. Analysis of the Large Deformation Mechanism of Roadway Surrounding Rock

After excavation of the roadway, the surrounding rock stress will redistribute, the deformation of the surrounding rock occurs while the surrounding rock stress exceeds the support strength of the roadway, and the plastic yield zone of the surrounding rock is formed. The basic driving force of the surrounding rock deformation is mainly the geo-stress and mining stress; the mechanical characteristics of surrounding rock have an important influence on the deformation and failure of roadway surrounding rock, such as elasticity modulus, Poisson's ratio, tensile strength and internal friction angle [42,43]. According to the deformation and mechanical properties analysis of the roadway surrounding rock for the Shishan Coal Mine, there are many influencing factors for the deformation and failure of roadway surrounding rock, but it is mainly reflected in these aspects:

- (1) Compared to the shallow roadway, the geological condition of the deep soft rock roadway is more complex and changeable, such as high geo-stress, developed joint fissures and unloading crack intensive belt. The geological condition difference usually brings the different technical problems of roadway support [32].
- (2) The direct roof is mainly mudstone or sandy mudstone, and the bedding has a certain development with abundant micro-cracks. When the roof produces a certain deflection, the rapid opening of micro-cracks leads to air entering the rock surface and makes the roof become plate-shaped, and the rock part of the mass of the roof loses its bearing capacity, further leading to the occurrence of roof failure.
- (3) Because there is not enough pre-tightening force on the roadway roof, the roof stress is transmitted to both sides by the roof after roadway excavation. The deformation of the roof increases the horizontal pressures on both sides of the roadway under the condition of a certain lateral pressure coefficient. In this way, the peak value of

pressure reaches the roadway sides, making the side wall of the roadway produce a plastic zone, and the overall outward displacement will occur once the side wall of the roadway cannot resist the expansion pressure.

- (4) The support mode is not very reasonable and synergistic because this design mechanically copies the adjacent roadway support scheme of the U-shaped steel flexible support. However, in practical application, the U-shaped steel shrinkage cannot play a major role due to the deformation of the trapezoidal bracket leg. While the weathered surrounding rock is splintered under pressure, passive support alone cannot meet the requirement of surrounding rock support stability. Thus, the full-space synergy control technology should be used to improve the self-bearing capacity of the surrounding rock.

### 3. Method of Full-Space Synergy Control

The support scheme and parameters of the roadway are primarily determined by the geo-stress condition and mechanical characteristics of the surrounding rock. They are also two key factors to realizing the targeted and effective control of roadway surrounding rock deformation under the different conditions [44]. If the choice of support form and parameters is unreasonable, it will result in one of the two extremes that follow:

- (1) The supporting strength is too high, which will not only waste support materials but also affect the excavation speed of the roadway.
- (2) The supporting strength is not enough, which cannot effectively control the deformation of the roadway surrounding rock and can lead to roof collapse, rib spalling, floor heave and other disasters.

To realize targeted and effective control of the roadway surrounding rock under different conditions, the full-space synergy control idea and method are applied in this study. Its core idea is that the choice of support mode in the project is based on the failure degree of the roadway surrounding rock [40]. The collaborative control operation technology of the coal mine roadway is mainly by changing the surrounding rock property and active unloading pressure to give full play to the self-bearing capacity of the surrounding rock. The basic principles include six aspects: full-space support, high-strength yielding, energy-releasing, rigid-flexible synergy, dynamic monitoring and local reinforcement. The roadway support mode can be divided into four types: one is the conventional buried depth mining roadway, the pretension rock bolt support is usually applied to control the roadway surrounding rock deformation due to the limited driving force of surrounding rock deformation; the second is the conventional buried depth large roadway, it generally needs to perform the shotcrete-bolt reinforcement technique; the third is the deep mining roadway, the common support method is active and passive coupling support with high preload bolt, wire mesh and shotcrete, and there is a curved roof to reduce local stress concentration; the fourth is the deep large roadway, the combined support with high strength and preload cable bolt, grouting modification, steel pipe shotcrete bracket and shotcrete is often applied to effectively control the large deformation of roadway surrounding rock. After the completion of roadway support, it needs to conduct dynamic monitoring of the surrounding rock deformation to master the information of the surrounding rock and perform the strengthened local support in potential failure risk areas.

For the full-space synergy control technology of the coal mine roadway, the optimization design of support parameters is the key factor in controlling the stability of the surrounding rock. The optimization methods of the supporting parameters can usually be divided into five types: engineering analogy, theoretical analysis, numerical modeling, field measurement and comprehensive design method [24,45]. This paper takes the deep mining roadway as an example to study its optimal support design, so the design of bolt parameters optimization is the key to increasing the self-bearing capacity and the stability of the surrounding rock. The bolt parameter optimization includes bolt diameter, bolt length, bolt interval and bolt pretension. Figure 3 is the process of support mode and

parameter optimization in coal mine roadways using the full-space synergy control idea and method.

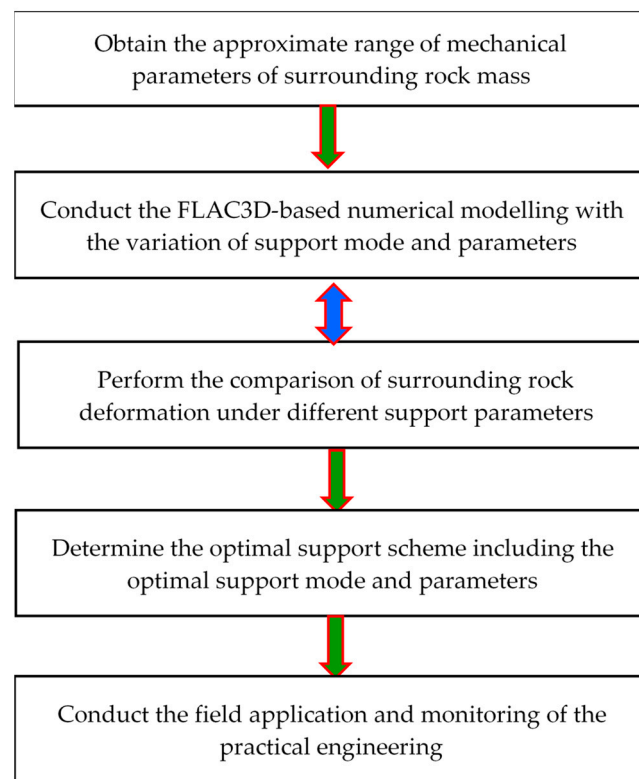


**Figure 3.** The optimization process of roadway support mode and parameters.

#### 4. Basic Theoretical Model

The finite difference method is adopted to analyze the stability of roadway surrounding rock with variation in the bolt parameters. An explicit finite difference program is used to solve the governing differential equation of the solving field. The mixed element discrete model is used to numerically analyze the mechanical behavior of a continuous three-dimensional medium, such as material yield, material large deformation and the excavation process of the rock mass.

##### 4.1. Equation of Motion

To describe the mathematical relationship between force and displacement (including velocity) of the rock mass, according to the momentum principle, the motion equation of continuous solid medium with the Cauchy method is written as follows:

$$\rho \frac{dv_i}{dt} = \frac{d\sigma_{ij}}{dx_j} + \rho b_i \quad (1)$$

where  $\rho$  is the mass density of the medium,  $v_i$  is the component of the velocity vector,  $b_i$  is the component of the body force vector per unit mass,  $t$  is time,  $\sigma_{ij}$  is the component of the stress tensor and  $x_i$  is the component of the coordinate system position. In the mathematical model, the law mainly expresses the motion displacements of an elementary volume of the medium from the forces applied to it.

##### 4.2. Constitutive Equation of Rock Mass in Incremental Form

The constitutive equation is used to describe the relationship between stress and strain of the rock mass. Because the stress and strain distribution of geotechnical engineering are

related to the construction process, the nonlinear constitutive equation of the rock mass in incremental form is expressed:

$$d\sigma_{ij} = \left( K - \frac{2}{3}G \right) d\sigma_{kk}\delta_{ij} + 2Gd\epsilon_{ij} \quad (2)$$

where  $d\sigma_{ij}$  is the stress tensor increment,  $d\epsilon_{kk}$  and  $d\epsilon_{ij}$  are the normal strain and shear strain tension increments, respectively,  $K$  and  $G$  are the bulk modulus and shear modulus, respectively, and they are connected with the elastic modulus  $E$  and Poisson's ratio  $\nu$  as follows:

$$K = \frac{E}{3 \times (1 - 2\nu)}, G = \frac{E}{2 \times (1 + \nu)} \quad (3)$$

#### 4.3. Theoretical Model of Anchored Surrounding Rock

In this study, the screw thread steel bolt is chosen to install in the roadway surrounding rock. Each bolt's structural element is defined by its geometric, material and grout properties. Generally, the full-length pretensioned anchoring of bolts is called the full-stress anchoring of bolts, rather than the term for full-length anchoring of bolts [38,46]. Pretensioned bolts can be fully anchored, and they can also be left anchored for part of their length. The entire working process of anchoring the interface of the bolts can be divided into three deformation stages, elastic deformation, strain softening and residual strength [37]. Figure 4 is the mechanical representation of the fully anchored reinforcement element system; the friction force between the bolt and the anchoring agent is expressed by the reinforcement nodal point with cohesive strength and shear strength. The large-area contact between shotcrete and the surrounding rock and bolt can penetrate into the rock mass to a certain extent so as to coordinate the deformation of the surrounding rock and act together with the surrounding rock to form the supporting arch.

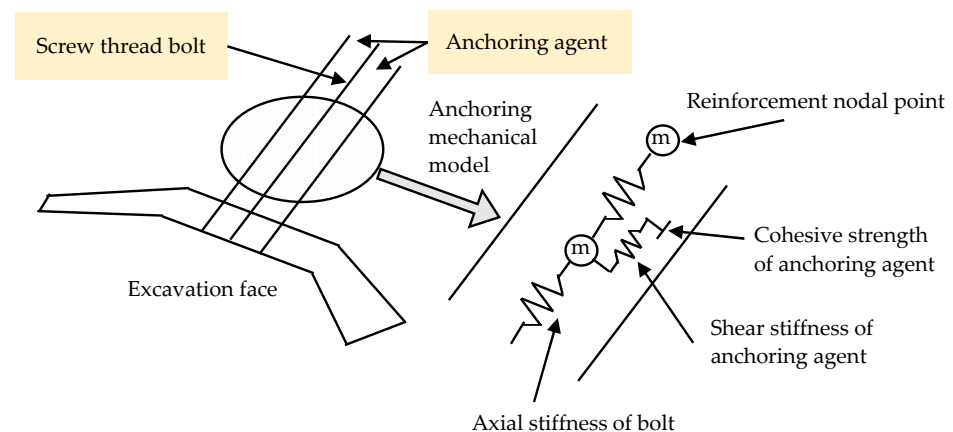


**Figure 4.** The mechanical representation of the fully anchored reinforcement element system.

Because the length of the bolt itself is much larger than its diameter, the bolt belongs to the member in mechanics, and there are mainly two functions: tensile and shear resistance. The compression resistance and bending resistance of the bolt body are very small and can be ignored. For the anchoring agent, the major function is divided into two aspects: first, the bolt body is bonded with the wall of the borehole so that the bolt bears tension in the opposite direction when the rock stratum moves; second, it can act together with the rock mass to resist shear and prevent the rock stratum sliding when rock stratum displacement occurs.

##### 4.3.1. Anchoring Stress

An axial force comprises axial force in the reinforcement and shear forces contributed by shear interaction along the anchoring annulus. Therefore, axial displacements are

calculated by integrating the nodal accelerations using the axial force of the reinforcing element and shear forces of reinforcement. Figure 5 is a mechanical schematic diagram of an elastic-viscoelastic element for the anchored-bolt system, and it is also called the Kelvin–Voigt model [47]. In this model, the total strain  $\varepsilon$  is comprised of the instantaneous elastic strain  $\varepsilon_1$  and the Kelvin strain body  $\varepsilon_2$  as follows:

$$\varepsilon = \varepsilon_1 + \varepsilon_2 \tag{4}$$

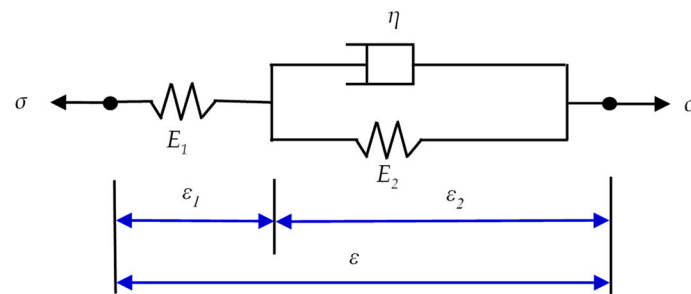


Figure 5. The mechanical model of the improved element.

For instantaneous elastic strain:

$$\varepsilon_1 = \frac{\sigma}{E_1} \tag{5}$$

For Kelvin strain bodies:

$$\varepsilon_2 = \frac{\sigma}{E_2} - \frac{\eta}{E_2} \dot{\varepsilon}_2 \tag{6}$$

where  $\sigma$  is the total stress,  $\eta$  is viscosity coefficient,  $\dot{\varepsilon}$  is strain rate and  $E_1$  and  $E_2$  are the bolt elastic modulus and anchored rock mass elastic modulus, respectively.

Equations (5) and (6) are substituted into Equation (4) to derive the constitutive equation of the elastic-viscoelastic model of anchored bodies:

$$\varepsilon = \frac{E_1 + E_2}{E_1 \cdot E_2} \sigma - \frac{\eta}{E_2} \dot{\varepsilon} + \frac{\eta}{E_1 \cdot E_2} \dot{\sigma} \tag{7}$$

The initial condition is:

$$\varepsilon = \frac{\sigma_0}{E_1}, \text{ When } t = 0 \tag{8}$$

When time  $t = 0$ , assuming the applied stress  $\sigma = \sigma_0 = \text{constant}$ , the strain  $\varepsilon = \varepsilon_0 = \text{constant}$  and the strain rate  $\varepsilon' = 0$ , Equation (7) can be solved as follows:

$$\sigma(t) = \left( \frac{E_1 \cdot E_2}{E_1 + E_2} + \frac{E_1^2}{E_1 + E_2} e^{-\frac{E_1 + E_2}{\eta} t} \right) \varepsilon_0 \tag{9}$$

#### 4.3.2. Surrounding Rock Convergence Ratio and Bolt Parameters Design

The relative convergence of surrounding rock displacement can not only be conveniently obtained but also accurately reflects the real state of the surrounding rock. Therefore, it is usually used to control the maximum permissible convergence displacement values of the surrounding rock; its definition is the ratio between the absolute value of radial convergence displacement in each control point of the roadway and the half of the radial distance in the closed space. For an arched roadway, the displacement convergence ratio of the vault is expressed as:

$$r_v = \frac{U_r}{r} \tag{10}$$

where  $r_v$  is the vault convergence ratio,  $U_r$  is the vault radial convergence displacement and  $r$  is the roadway vault radius.

The displacement convergence ratio of the two walls is expressed:

$$r_s = \frac{U_s}{d} \quad (11)$$

where  $r_s$  is the convergence on both sides of the roadway,  $U_s$  is the convergence displacement of the roadway's two sides and  $d$  is the distance between the two sides of the roadway.

An investigation showed that the roadway surrounding rock would lose stability when the displacement convergence ratio was greater than or equal to 2% [48–50].

Bolt support is the major development direction in deep mining roadway support, and it is proposed and developed on the basis of the co-bearing theory. The bolt support can greatly improve the support effect by changing the original passive support into active support; this is why the bolt-anchorage body model is called the improved model. This paper uses the suspension theory to perform the design of bolt parameters. The estimation formula of the bolt length can be expressed as:

$$L = kR + L_1 + L_2 \quad (12)$$

where  $L$  is the bolt length,  $k$  is the safety coefficient and generally takes 1 to 3,  $L_1$  is the length of anchoring in stable rock beyond the loose range, generally, 0.3 to 0.4 m, and  $L_2$  is the exposed length of the bolt in the roadway.  $R$  is the loose zone radius of the surrounding rock as follows:

$$R = R_0 \left[ (1 - \sin \varphi) \frac{\sigma_z + C \cot \varphi}{C \cot \varphi} \right]^{\frac{1 - \sin \varphi}{2 \sin \varphi}} \quad (13)$$

where  $R_0$  is the radius of the outer circle of the roadway,  $\sigma_z$  is the gravity stress of the overlying stratum,  $C$  is adhesion and  $\varphi$  is the internal friction angle.

The estimation formula of row spacing and column spacing is expressed as:

$$a = \sqrt{\frac{F_T}{Rk\gamma}} \quad (14)$$

where  $a$  is the bolt interval,  $F_T$  is the anchorage force of the roof design and  $\gamma$  is the weight of the roof's surrounding rock.

## 5. Numerical Simulation Analysis of Surrounding Rock Stability

### 5.1. FLAC3D Numerical Computation Model

FLAC3D is used to establish the numerical calculation model to analyze the deformation of the roadway surrounding rock during roadway excavation. Figure 6 is a plane calculation model with a side of 60 m × 90 m as the excavation face and an exaggerated diagram of the excavation roadway. The excavation depth of the calculation model is programmed to 30 m. Thus, as shown in Figure 7, a cube FLAC3D numerical simulation model with a model size of 30 m × 60 m × 90 m is created for a study of the stability control of the roadway surrounding rock.

As shown in Figure 6, the coordinate origin takes the center position of the roadway, the X-axis is directed to the right, the Z-axis is directed to the upper and the Y-axis is pointing in the excavation direction. The two sides of the model are constrained in the horizontal direction, and the bottom of the model is fixed. The roadway excavation is simulated based on the actual size with a semicircular arch and a straight wall of diameter of 3.2 m and height of 1.6 m. The top surface of the calculation model employs a stress boundary condition, and the gravity stress of the overburden is used as the vertical stress applied to the top surface; the expression is as follows:

$$\sigma_{cz} = \bar{\gamma} \cdot \bar{h}_0 \quad (15)$$

where  $\sigma_{cz}$  is the gravity stress of the overburden,  $\bar{\gamma}$  is the average unit weight of overburden and  $\bar{h}_o$  is the average depth of overburden.

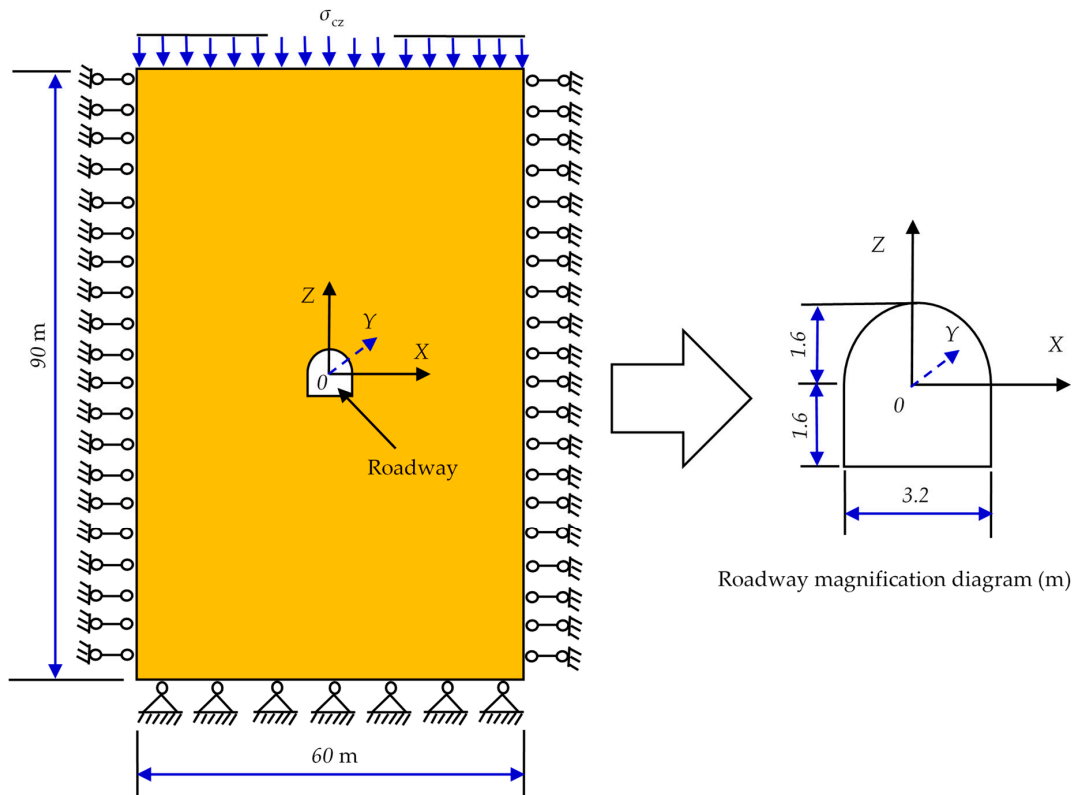


Figure 6. The boundary condition of numerical calculation model and roadway geometric size.

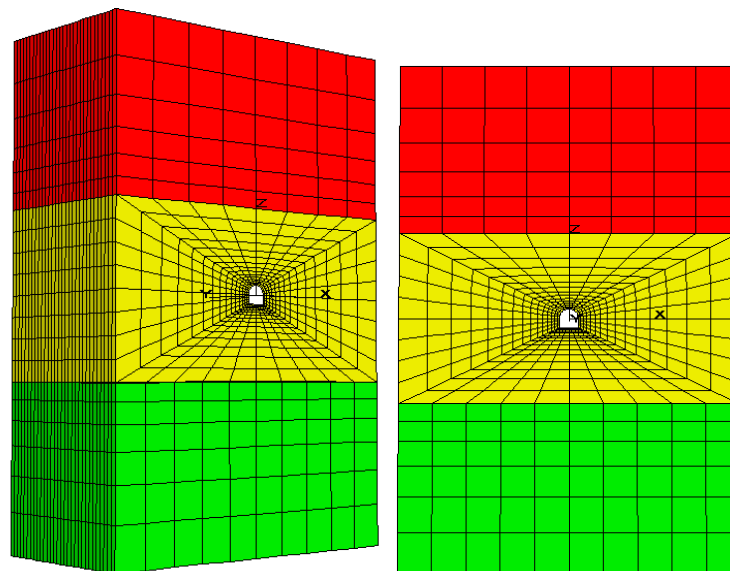


Figure 7. The three-dimensional numerical model based on FLAC3D.

### 5.2. Input Parameters of Numerical Computation Model

Because the deep roadway is in a very complex and changeable geological environment in practical engineering, there are many factors that affect the stability of the roadway surrounding rock, but it is impossible to completely consider all influencing factors when performing the numerical simulation. As shown in Figure 7, to effectively conduct the numerical simulation analysis, the calculation model is simplified as a three-layer homoge-

neous isotropic model. By experimental measurement, theoretical computation, parameters inversion and other methods, the average unit weight and average thickness of overburden rock mass are considered as  $24.5 \text{ kN/m}^3$  and  $472.37 \text{ m}$ , respectively, and the other experimental parameters of the numerical modeling are shown in Table 1. The Mohr–Coulomb yield criterion is used to analyze the material yield and failure situation, and the expression is as follows:

$$f_s = (\sigma_1 - \sigma_3) - 2C \cos \varphi - (\sigma_1 + \sigma_3) \sin \varphi \quad (16)$$

where  $\sigma_1$  and  $\sigma_3$  are the maximum principal stress and the minimum principal stress, respectively, the shear failure will occur when the function  $f_s < 0$ .

**Table 1.** The mechanical parameters of the surrounding rock mass and coal.

Location	Density	Shear Modulus	Bulk Modulus	Strength of Extension	Cohesion	Internal Friction Angle	Dilation Angle
	$\rho/\text{kg}\cdot\text{m}^{-3}$	$G/\text{MPa}$	$K/\text{Mpa}$	$\sigma_t/\text{Mpa}$	$C/\text{Mpa}$	$\varphi/^\circ$	$\psi/^\circ$
Roof layer	2400	3836	4363	0.70	1.30	28	0
Coal seam	1400	1600	3467	0.20	0.60	28	0
Floor layer	2510	1670	2227	0.40	1.50	30	5

### 5.3. Determinization of Modeling Scheme

The optimal scheme is obtained through statistical analysis and numerical simulation analysis, which needs to be verified by experiments to ensure that the optimal scheme is consistent with the actual situation. In this study, based on the actual measured data information of rock mass mechanics in the Shishan Coal Mine and some pre-design roadway support schemes, roadway excavation without support and bolt-shotcrete net combined support with the different bolt parameters are simulated to study the deformation and failure mechanism of the roadway surrounding rock. By comparison, it is proved that the supporting scheme is more reasonable, which makes a proposal for the optimization design of roadway support in the Shishan Coal Mine.

This study applies the whole section excavation of the roadway step by step, and the computation is conducted every 3 m of the excavation until the model of 30 m is fully excavated. The displacement of the roadway surrounding rock at excavation depth without support is in Table 2. Figure 8 is the deformation of the roadway surrounding rock over the excavation length in the absence of support. Although the simulation displacement results increase with the tunneling of the working face, the deformation values are very small for every 3 m excavation after the roadway is excavated 12 m. Therefore, this study takes the deformation section of the roadway after 12 m excavation as the research object in the following numerical simulation.

**Table 2.** Displacement of roadway surrounding rock with excavation depth without support.

Excavation Length	Roof Subsidence	Floor Heave	Roof-to-Floor Convergence	Left Displacement	Right Displacement	Left-to-Right Convergence
(m)	(mm)	(mm)	(mm)	(mm)	(mm)	(mm)
3	−28.943	20.098	49.041	24.068	−24.027	48.095
6	−34.29	23.839	58.129	30.329	−30.308	60.637
9	−36.579	26.346	62.925	33.357	−33.332	66.689
12	−37.877	27.485	65.362	34.795	−34.772	69.567
15	−38.618	27.947	66.565	35.517	−35.495	71.012
18	−39.125	28.108	67.233	35.934	−35.912	71.846
21	−39.534	28.135	67.669	36.215	−36.193	72.408
24	−39.896	28.09	67.986	36.427	−36.405	72.832
27	−40.255	28.011	68.266	36.615	−36.594	73.209
30	−40.77	29.092	69.862	37.257	−37.254	74.511

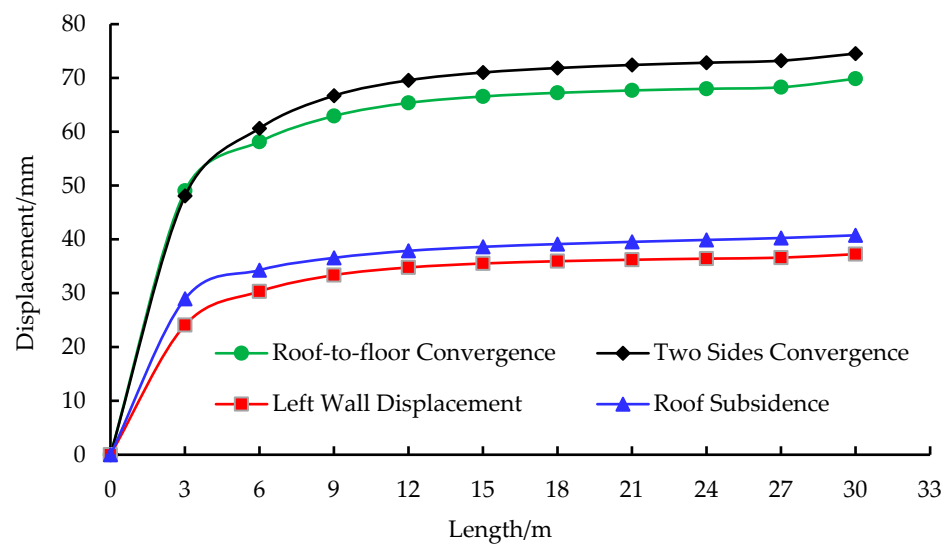


**Figure 8.** Deformation of roadway surrounding rock with excavation length without support.

#### 5.4. Simulation Analysis of Surrounding Rock Deformation based on Orthogonal Design Method

##### 5.4.1. Theory of Orthogonal Experimental Design

Orthogonal experimental is a method used in multi-factor tests [49]. It uses mathematical statistics and the orthogonality principle to select some representative and typical test points, which are required to have the characteristics of uniformity and orderliness. It usually uses the orthogonal tables to arrange experiments scientifically and rationally to obtain the optimal results in as few experiments as possible. There are two basic requirements for orthogonal experimental design: (1) any one of these factors has the same number of occurrences at different levels in the experiment; (2) the level combination of any two factors will occur in the experiment at the same number of the occurrence frequency. To reflect the general situation of each influencing factor and level of the index comprehensively, the orthogonal experimental table is designed by the following equation:

$$T = S_n(L^m) \quad (17)$$

where  $S$  is the scheme of the orthogonal experiment,  $n$  is the number of the experiment,  $L$  is the number of levels and  $m$  is the number of influence factors of the experiment.

##### 5.4.2. Orthogonal Design of Sensitivity Analysis for Bolt Parameters

The sensitive analysis of roadway surrounding rock deformation is conducted to optimize the support parameters in this study. The main support parameters of roadway bolt support in stope are bolt diameter, bolt length, bolt interval and bolt pretension. These four parameters are taken as four factors of orthogonal experiment, and there are four levels for each factor (i.e.,  $S_n(4^4)$ ). Table 3 is the changing situation in factors and levels. The technological process of roadway excavation and support installation is conducted incrementally. For each step, excavation is advanced 3 m, and the pre-support concrete shield, bolts, shotcrete and thick concrete liner are installed at the specified distance from the roadway face. The input mechanical properties of the bolt in the numerical simulation are given in Table 4.

**Table 3.** The factor scheme of the orthogonal numerical simulation experiment.

Level	Bolt Diameter	Bolt Length	Bolt Interval	Bolt Pretension
	A (mm)	B (mm)	C (mm)	D (kN)
1	18	1800	700	60
2	20	2000	800	80
3	22	2200	900	100
4	25	2400	1000	120

**Table 4.** The mechanical parameters of the bolt in numerical modeling.

Bolt Diameter	Elastic Modulus	Bolt Section Aear	Aperture Circumference	Grout Bond Stiffness	Gout Cohesive Strength	Bolt Tensile Capacity
(mm)	(Gpa)	(m <sup>2</sup> )	(m)	(N/m/m)	(N/m)	(kN)
18	200	0.254	0.13188	$26.8 \times 10^6$	$2.1 \times 10^6$	$1.36 \times 10^5$
20	200	0.314	0.13188	$30.6 \times 10^6$	$2.3 \times 10^6$	$1.65 \times 10^5$
22	450	0.38	0.13188	$35 \times 10^6$	$2.5 \times 10^6$	$2.50 \times 10^5$
25	450	0.491	0.13188	$43.8 \times 10^6$	$2.8 \times 10^6$	$3.10 \times 10^5$

Since this study applies FLAC3D numerical simulation to analyze the influence of bolt support parameters for the deformation and failure of the roadway surrounding rock, the maximum displacement of the roof and floor, the maximum displacement of the left and right sides and the size of plastic zone for each test scheme are selected as the evaluation index to find the optimal support design for the roadway. The number of shear and tensile yield elements is used to express the plastic yield zone size of the surrounding rock. Table 5 is designed for 64 schemes of the orthogonal experiment. In Table 5, “+” represents that the displacement direction is consistent with the coordinate direction, “−” represents that the displacement direction is not consistent with the coordinate direction.

**Table 5.** Bolt anchoring experimental design of orthogonal numerical simulation.

No.	Influencing Factor of Bolt				Simulation Results of Surrounding Rock Deformation			
	Diameter (mm)	Length (mm)	Interval (mm)	Pretension (kN)	Subsidence (mm)	Heave (mm)	Side Convergence (mm)	Plasticity Number (mm)
1	18	1800	700 × 700	60	−24.185	+25.730	52.854	61
2	18	1800	800 × 800	60	−24.205	+25.735	52.940	55
3	18	1800	900 × 900	80	−23.371	+25.067	52.271	52
4	18	1800	1000 × 1000	80	−24.275	+25.755	53.071	64
5	18	2000	700 × 700	100	−24.183	+25.734	52.834	61
6	18	2000	800 × 800	100	−24.211	+25.741	52.944	55
7	18	2000	900 × 900	120	−24.348	+25.762	53.146	57
8	18	2000	1000 × 1000	120	−24.277	+25.758	53.061	58
9	18	2200	700 × 700	60	−24.206	+25.740	52.813	61
10	18	2200	800 × 800	60	−24.225	+25.739	52.908	61
11	18	2200	900 × 900	80	−24.258	+25.752	52.984	61
12	18	2200	1000 × 1000	80	−24.271	+25.755	53.250	63
13	18	2400	700 × 700	100	−24.178	+25.737	52.809	58
14	18	2400	800 × 800	100	−24.213	+25.743	52.881	58
15	18	2400	900 × 900	120	−24.256	+25.754	52.970	61
16	18	2400	1000 × 1000	120	−24.280	+25.755	53.022	61
17	20	1800	700 × 700	60	−24.155	+25.721	52.798	60
18	20	1800	800 × 800	60	−24.175	+25.726	52.894	59
19	20	1800	900 × 900	80	−24.242	+25.747	52.996	61
20	20	1800	1000 × 1000	80	−24.248	+25.753	53.051	62

Table 5. Cont.

No.	Influencing Factor of Bolt				Simulation Results of Surrounding Rock Deformation			
	Diameter (mm)	Length (mm)	Interval (mm)	Pretension (kN)	Subsidence (mm)	Heave (mm)	Side Convergence (mm)	Plasticity Number (mm)
1	18	1800	700 × 700	60	−24.185	+25.730	52.854	61
2	18	1800	800 × 800	60	−24.205	+25.735	52.940	55
3	18	1800	900 × 900	80	−23.371	+25.067	52.271	52
4	18	1800	1000 × 1000	80	−24.275	+25.755	53.071	64
5	18	2000	700 × 700	100	−24.183	+25.734	52.834	61
6	18	2000	800 × 800	100	−24.211	+25.741	52.944	55
7	18	2000	900 × 900	120	−24.348	+25.762	53.146	57
8	18	2000	1000 × 1000	120	−24.277	+25.758	53.061	58
9	18	2200	700 × 700	60	−24.206	+25.740	52.813	61
10	18	2200	800 × 800	60	−24.225	+25.739	52.908	61
11	18	2200	900 × 900	80	−24.258	+25.752	52.984	61
12	18	2200	1000 × 1000	80	−24.271	+25.755	53.250	63
13	18	2400	700 × 700	100	−24.178	+25.737	52.809	58
14	18	2400	800 × 800	100	−24.213	+25.743	52.881	58
15	18	2400	900 × 900	120	−24.256	+25.754	52.970	61
16	18	2400	1000 × 1000	120	−24.280	+25.755	53.022	61
17	20	1800	700 × 700	60	−24.155	+25.721	52.798	60
18	20	1800	800 × 800	60	−24.175	+25.726	52.894	59
19	20	1800	900 × 900	80	−24.242	+25.747	52.996	61
20	20	1800	1000 × 1000	80	−24.248	+25.753	53.051	62

#### 5.4.3. Orthogonal Experimental Results and Analysis

Figure 9 is the roof deformation situation of the roadway surrounding rock under four influencing factors. Table 6 is the average value of vault subsidences at the maximum subsidence point and its range under four influence factors. Table 7 is the average value of two sides' convergence at the maximum displacement point and its range under four influencing factors. According to the results from Figure 7, Tables 6 and 7, it can be seen that (1) the bolt diameter has a similar influence on that of bolt pretension, the roof-to-floor and two sides convergence decrease with the increase in the bolt diameter and bolt pretension, and the effect of pretension on the roof-to-floor convergence tend to be stable after pretension is 80 kN; (2) the roof-to-floor and two sides convergence decrease with the increase in the bolt length, but the effect of the bolt length on the roof-to-floor convergence is constant when the bolt length increases to a certain value where its diameter is larger than the loose circle of the roadway surrounding rock; (3) the roof-to-floor convergence first decreases and then increases with the increase in the bolt interval, but there is a very small difference between an internal of 800 mm × 800 mm and an internal of 900 mm × 900 mm; (4) two sides convergence increases with the increase in the bolt interval, and it obviously increases when the internal is greater than the internal of 900 mm × 900 mm. The results illustrate that the influence law of each factor on the subsidence of the roadway roof is essentially the same as engineering practice, albeit slightly different in size because the practical engineering converge is a constantly changing quantity and also a function of time.

Figure 10 is the variation curve of the plastic zone size of the roadway surrounding rock under four different influencing factors. Table 8 is the number and range of the plastic yield zone around the roadway surrounding rock under four different factors. From the results in Figure 10 and Table 8, it can be seen that (1) bolt diameters have a similar result as the interval; the number of plastic yield zone first increases, then decreases and then increases with the increase in diameter and interval; (2) bolt length and pretension have a similar effect on the number of the plastic yield zone under the different influencing

factors, they increase and then tend to a relatively stable level. The results illustrate that the bolt diameter and interval have a relatively large influence on the plastic yield zone, and the bolt length and pretension are relatively small, which is basically in accordance with practical engineering.

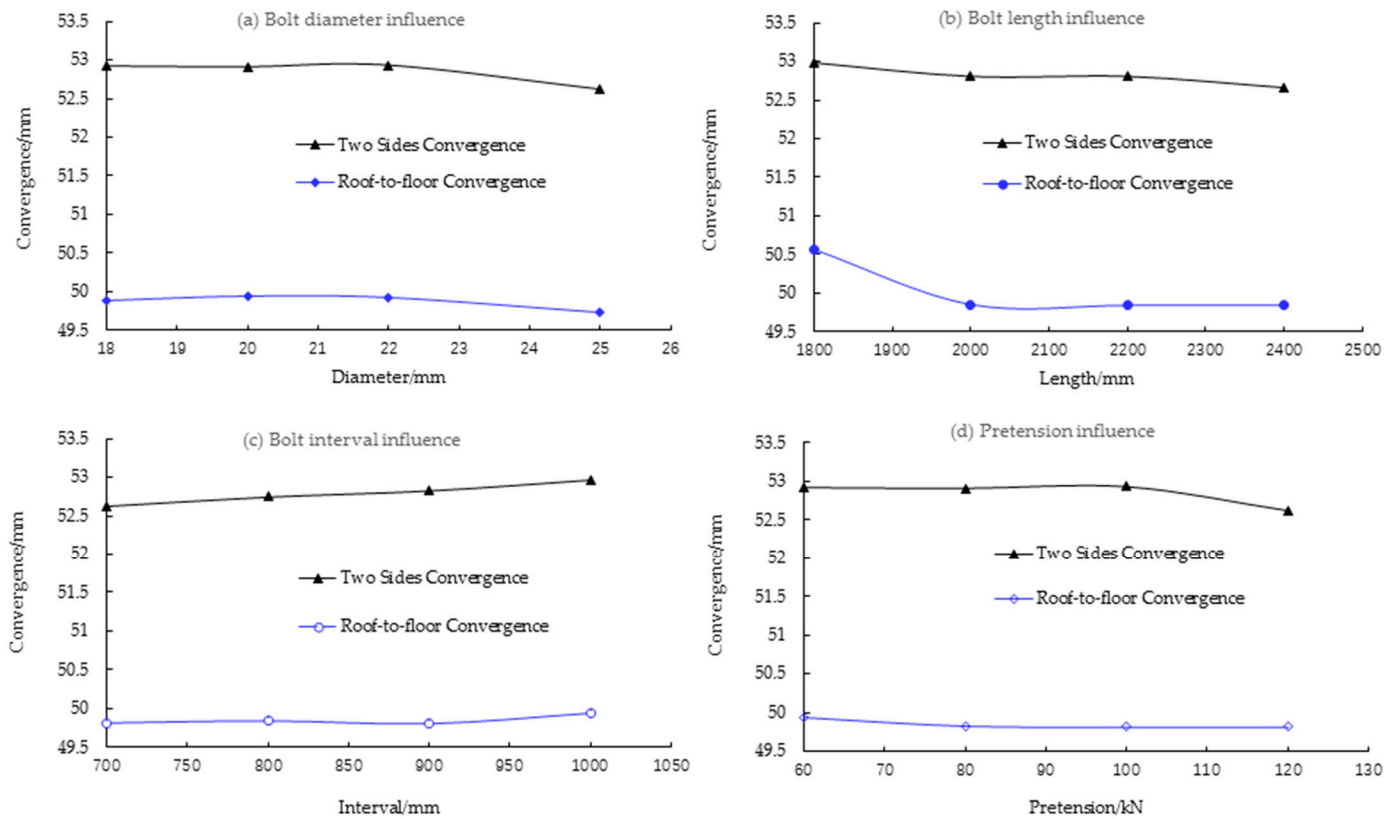


**Figure 9.** The variation curve of roadway convergence under the different influencing factors. (a) Bolt diameter influence; (b) Bolt length influence; (c) Bolt interval influence; (d) Pretension influence.

**Table 6.** Results and analysis of roof-to-floor convergence under four different factors.

Level Average	Roof-to-Floor Convergence at the Maximum Point (mm)			
	Bolt Diameter (mm)	Bolt Length (mm)	Bolt Interval (mm)	Bolt Pretension (kN)
1	49.89	50.57	49.81	49.93
2	49.95	49.85	49.84	49.83
3	49.93	49.84	49.8	49.82
4	49.73	49.84	49.95	49.82
Range	0.22	0.73	0.15	0.11

**Table 7.** Results and analysis of two sides convergence under four different factors.

Level Average	Two sides Convergence at the Maximum Point (mm)			
	Bolt Diameter (mm)	Bolt Length (mm)	Bolt Interval (mm)	Bolt Pretension (kN)
1	52.92	52.99	52.63	52.92
2	52.91	52.81	52.75	52.91
3	52.93	52.81	52.83	52.93
4	52.62	52.66	52.97	52.62
Range	0.31	0.33	0.34	0.31

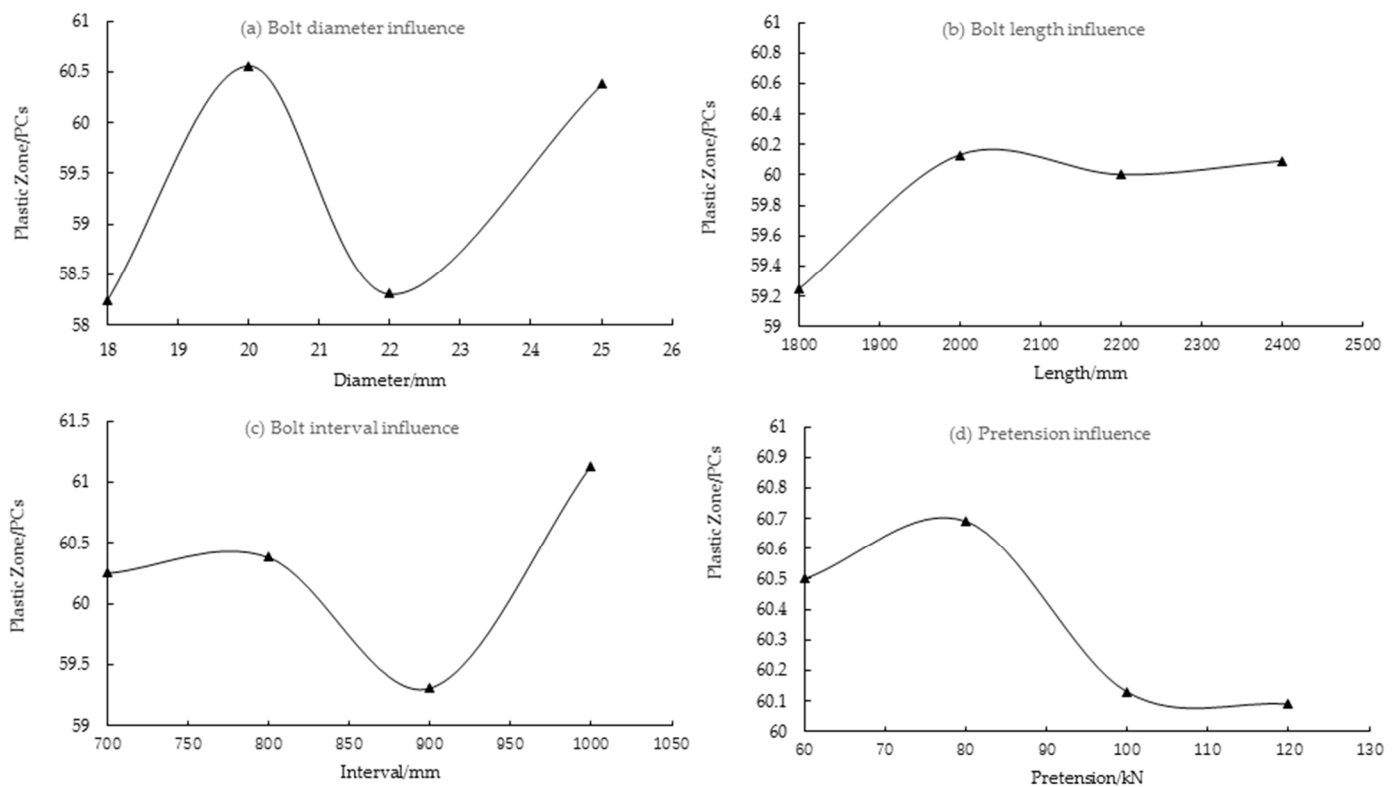


**Figure 10.** The variation of plastic zone size of surrounding rock under the different factors. (a) Bolt diameter influence; (b) Bolt length influence; (c) Bolt interval influence; (d) Pretension influence.

**Table 8.** Results and analysis of the plastic yield zone under four different influencing factors.

Level Average	Plastic Yield Zone (PCs)			
	Bolt Diameter (mm)	Bolt Length (mm)	Bolt Interval (mm)	Bolt Pretension (kN)
1	58.25	59.25	60.25	60.5
2	60.56	60.13	60.38	60.69
3	58.31	60	59.31	60.13
4	60.38	60.09	61.13	60.09
Range	2.31	0.88	1.82	0.6

## 6. Discussion of Field Test and Design

### 6.1. Determination of Support Mode and Parameters

This study was used to perform the analysis of the deformation and failure characteristics of deep soft rock roadways in the Shishan Coal Mine and its design of the support system. According to the comparison of the surrounding rock deformation between the unsupported roadway and bolt support roadway, it can be concluded that bolt support can coordinate with the deformation of the surrounding rock and interact with the surrounding rock to form the supporting arch by penetrating into the rock mass to a certain extent. The above investigation of the support mode and parameters illustrate that bolt support is an effective way to control the stability of the roadway surrounding rock, and the bolt support parameters of diameter 22 mm, length 2200 m, interval 700–900 mm and pretension 100 kN are the optimal match to control the deformation of the roadway surrounding rock.

To effectively improve the stress state and control the deformation development before supporting the surrounding rock, the early strength and close bounding property of shotcrete were used to give play to the self-bearing capacity and rapidly proved to support

resistance to the surrounding rock. Thus, this study applied the bolt-shotcrete combined support method with the different bolt parameters and the full-length anchorage. Figure 11 is the FLAC3D model of the bolt-shotcrete combined support. The shotcrete parameters are: Young's modulus  $E = 2.5$  Gpa, Poisson's ratio  $\nu = 0.25$ , thickness  $D = 100$  mm.

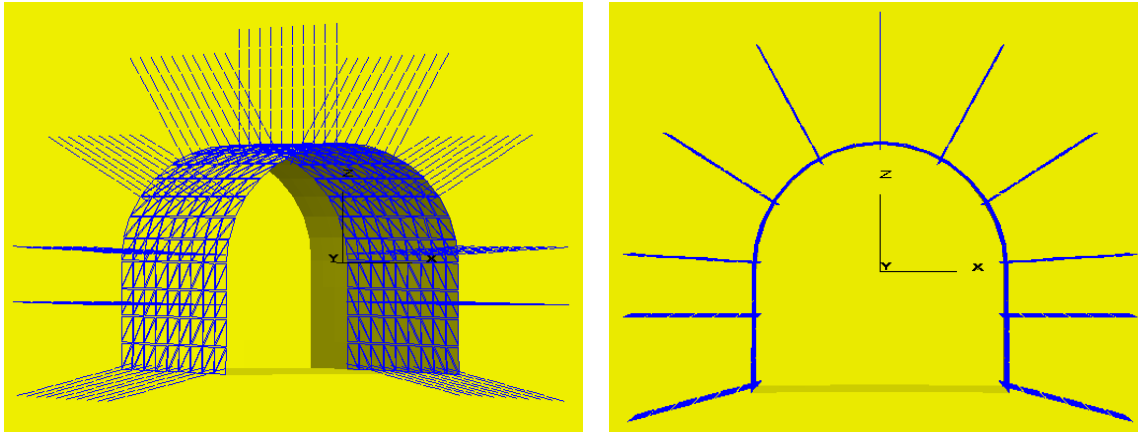


**Figure 11.** FLAC3D model of bolt-shotcrete net combined support.

#### 6.2. Numerical Modeling Analysis of the Roadway Surrounding Rock Deformation

To verify whether the bolt supporting parameters are optimal and the shotcrete is useful, a comparative analysis of the surrounding rock deformation in the test roadway is performed. Figure 12 is the roof and floor displacement contour of the test roadway at an excavation depth of 12 m. From Figure 12(left), it can be seen that the maximum roof subsidence and floor heave are more than 35 and 25 mm, respectively, for no supporting excavation roadway, especially the roof subsidence is still more than 15 mm at a distance of about 4 m from the roadway vault, and the convergence ratio of the vault is  $2.2\% > 2\%$ , these results illustrate that a larger loose circle has been formed in the vault so that it will lose the stability and the roof falling accidents will easily occur without timely supporting. From Figure 12(right), it can be seen that the maximum roof subsidence is about 20 mm with bolt-shotcrete support, which decreases by 43%. Among them, the roof subsidence at a distance of about 4 m from the roadway vault also decreases by about 5.7 mm, and the convergence ratio of the vault is  $1.25\% < 2\%$ . Moreover, the floor heave with bolt-shotcrete support is also a significant decrease. The results illustrate that the bolt-shotcrete support can not only reinforce the loose circle of the roadway roof but also control the floor heave to a certain extent to ensure the stability of the surrounding rock.

Figure 13 is the two sides displacement contour of the test roadway at an excavation depth of 12 m. From Figure 13(left), it can be seen that the maximum two sides convergence exceeds 65 mm for no supporting excavation roadway, and the convergence ratio of the two sides is  $2.2\% > 2\%$ . The results show that rib spalling accidents easily occur without timely support. As shown in Figure 13(right), when the bolt-shotcrete combined support is applied, the maximum movement on both sides of the roadway can keep around 40 mm, and the convergence ratio of the two sides is  $1.3\% < 2\%$ . The results show that the bolt-shotcrete support can also effectively control the movement of the two sides of the roadway.

Figure 14 is the plastic elements contour of the roadway surrounding rock subjected to shear and tensile yield at an excavation depth of 12 m. As shown in Figure 14(left), the red and block elements are the plastic yield zone; these yield elements are mainly concentrated in the roof and two sides of the roadway in the absence of any support. The number of plastic yield zone elements is as high as 178; the plastic yield zone range of surrounding rock has been extended to nearly 7 m in the surrounding rock. Therefore, if the safety and long-term stability of the roadway want to be ensured, it will be necessary to carry out the roadway support in a timely manner. As shown in Figure 14(right), while the combined support pattern of bolt-shotcrete is adopted, the plastic yield zone at the roof

and the corner or two sides of the roadway is well controlled; this also means that the stress concentration problems of the roadway surrounding rock are addressed. The plastic yield zone range is obviously reduced and is less than 1 m. Thus, the optimization of the support pattern is also very important to control the plastic yield zone development of the roadway surrounding rock.

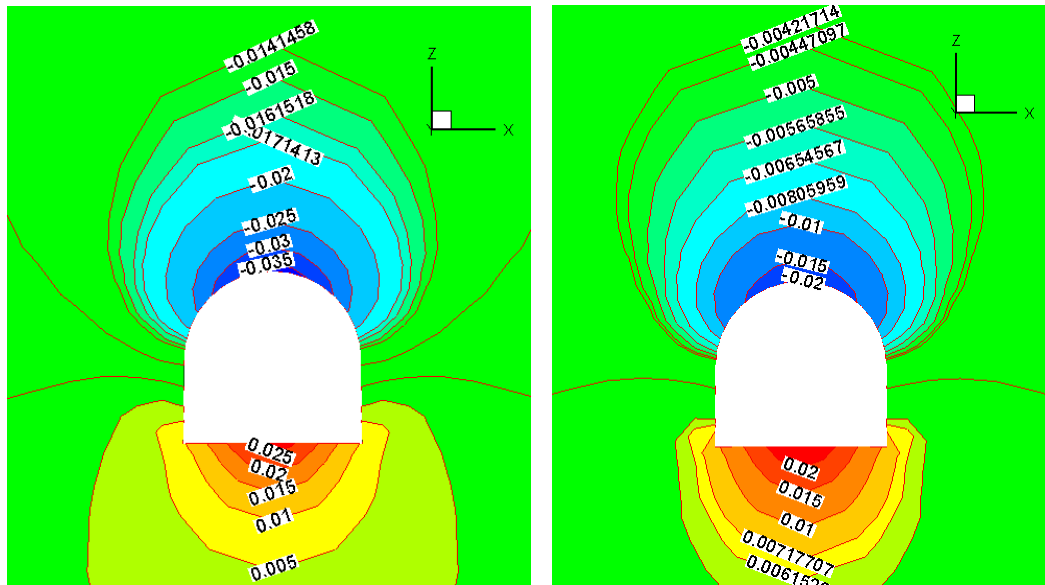


Figure 12. Roof and floor displacement contour of test roadway at an excavation depth of 12 m.

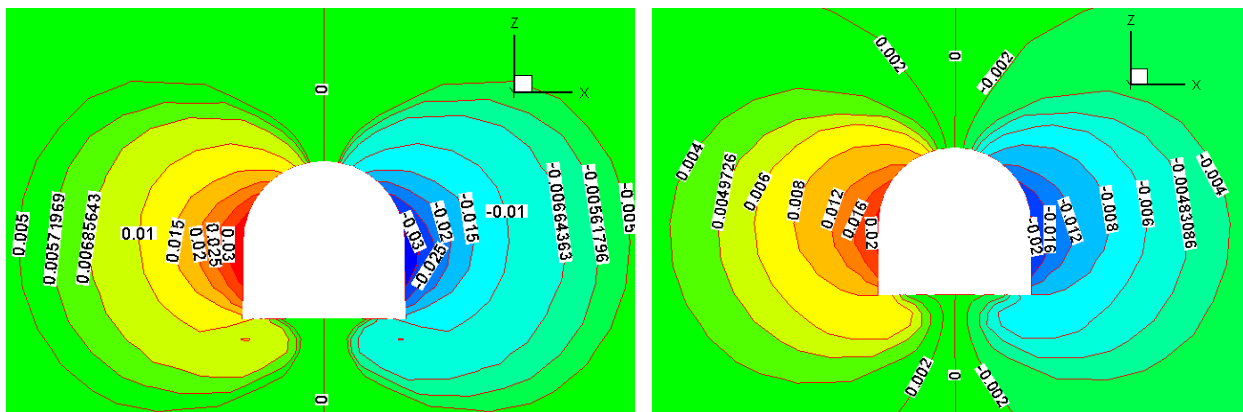


Figure 13. Two sides displacement contour of the test roadway at an excavation depth of 12 m.

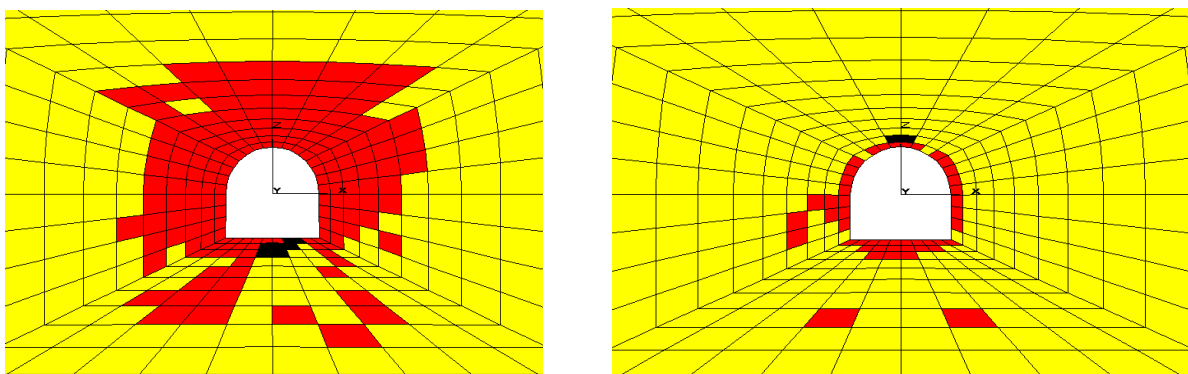


Figure 14. The plastic yield zone of roadway surrounding rock at an excavation length of 12 m.

### 6.3. Optimization Design Discussion of Support Structure

According to the above analysis of the convergence and plastic yield zone of the roof, floor and two sides of the roadway surrounding rock, the bolt-shotcrete combined support can effectively weaken the stress concentration at the corner of the roadway, and improve the self-bearing capacity of the surrounding rock at the corner and two sides of the roadway, so as to reduce the deformation of the roadway's two sides. The roof separation and subsidence caused by the failure of the surrounding rock can be effectively controlled by strengthening the roof, corners and two sides of the roadway. The deformation and plastic yield zone development of the surrounding rock are kept under the required range after performing bolt-shotcrete support, which illustrates that the selected support pattern and parameters can improve the stress environment and hold the further expansion of the loose zone of the surrounding rock, and ensure the stability and safety of the roadway surrounding rock. In order to take full advantage of these advantages of active support and full-space synergistic control idea and method, a W-shaped steel strip and wire mesh are used as supplemental support, the net type is a metal diamond mesh with a mesh of  $100\text{ mm} \times 100\text{ mm}$ , and the overlap length of the nets is  $100\text{ mm}$ . The row and line spacing are mainly between  $700$  and  $900\text{ mm}$ , and it can keep changing based on the practical design section size; the screw thread steel bolts are perpendicular to the surrounding face, and the bolts near the wall shall be tilted to a  $15^\circ$  angle with respect to the walls. The bolt-shotcrete net beam support structure of the test roadway is proposed in this study for the stability control of the roadway surrounding rock in the Shishan Coal Mine, which is shown in Figure 15.

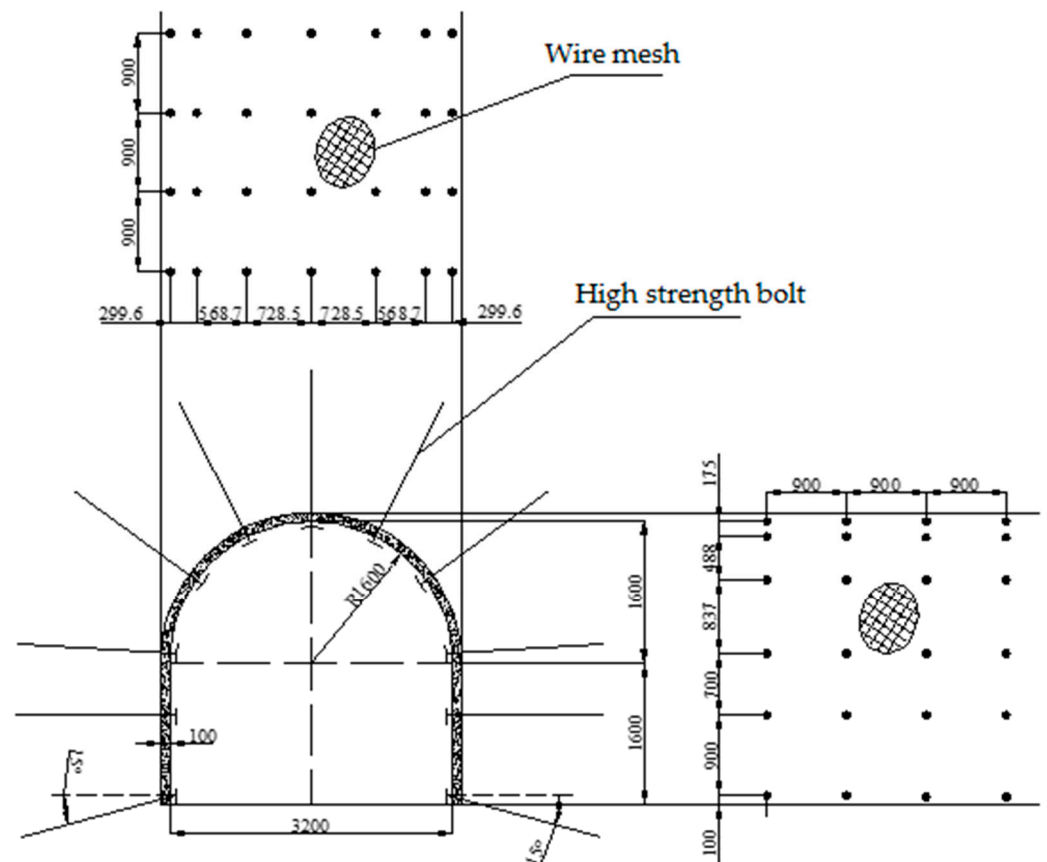


Figure 15. Bolt-shotcrete net support structure of the test roadway (mm).

## 7. Conclusions

Assisted by FLAC3D numerical modeling, the orthogonal numerical experiment with the experimental scheme of four factors and four levels was applied to study the influence

of bolt parameters and support patterns on the deformation and plastic yield zone of the roadway surrounding rock and realize the optimization of bolt support parameters, such as bolt diameter, bolt length and bolt interval. The full-stress anchoring technology of bolts was used to improve the initial pretension force. According to the full-space synergy technology, good results are acquired in this study, and the following conclusions are obtained:

- (1) The surrounding rock trend convergence deformation towards the interior of the roadway after roadway excavation. The convergent deformation of the surrounding rock drops sharply after conducting bolt support, which indicates that bolt support has an obvious control effect on the deformation and failure of the surrounding rock. However, the shotcrete support has a better effect on the plastic yield zone control than bolt support. Therefore, in the choice of optimization support pattern and parameters, it needs to take full advantage of different support schemes and give full play to their effectiveness to ensure the stability of the surrounding rock based on the practical engineering situation. This also can effectively ensure the stability of the roadway surrounding rock at a lower cost.
- (2) According to the mechanical and deformation characteristics of the surrounding rock, the bearing capacity of the surrounding rock can be significantly improved after adding a shotcrete net to the bolt support, and the influence on mining was also controlled. Therefore, when the bolt-shotcrete net beam support mode is adopted, the integrity and stability of surrounding rock mass in a deep roadway can be further improved because the metal mesh can support the rubble and/or coal between the bolt and maintain the integrity of the bolt support. In addition, the roof beam can assist the inclined bolts above the two sides to connect the roof and the two sides to prevent shear yield failure; this can effectively improve the stress state of the anchoring rock formation and increase the lateral extrusion pressure to enhance the bearing capacity of the composite arch support mode.
- (3) According to the comparison of the deformation data of the roadway surrounding rock from references [48–51], using the proposed arch support scheme is superior to the trapezoidal or rectangular metal support. The maximum displacements of the roof, floor and two sides are below 40 mm without support and are below 22 mm after applying for the bolt-shotcrete net support. As a result, the proposed optimization support scheme and parameters with the full-space synergy control technology and bolt application have great superiorities both in economy and technology.

**Author Contributions:** Methodology and conceptualization, S.Z. and S.Y.; writing—review, and project administration, S.Z.; formulation and software, S.Z. and S.Y.; investigation, S.Z. and S.Y.; writing—original draft preparation and editing, S.Z. and S.Y.; funding acquisition, S.Z. All authors have read and agreed to the published version of the manuscript.

**Funding:** This research was funded by the Natural Science Foundation of Henan Province of China (Grant No. 182300410160), and by the Training Project for Young Backbone Teachers of Higher Education of Henan (Grant No. 2018GGJS122).

**Institutional Review Board Statement:** Not applicable.

**Informed Consent Statement:** Not applicable.

**Data Availability Statement:** Data are contained within the article.

**Conflicts of Interest:** The authors declare no conflict of interest.

## References

1. He, M. Progress and Challenges of Soft Rock Engineering in Depth. *J. China Coal Soc.* **2014**, *39*, 1409–1417.
2. Liu, F.; Cao, W.J.; Zhang, J.M.; Cao, G.G.; Guo, L.F. Current Technological Innovation and Development Direction of the 14th Five-Year Plan Period in China Coal Industry. *J. China Coal Soc.* **2021**, *46*, 1–15. [[CrossRef](#)]
3. Wang, J.C.; Peng, S.S.; Li, Y. State-of-the-Art in Underground Coal Mining and Automation Technology in the United States. *J. China Coal Soc.* **2021**, *46*, 36–45. [[CrossRef](#)]

4. Świątek, J.; Janoszek, T.; Cichy, T.; Stoiński, K. Computational Fluid Dynamics Simulations for Investigation of the Damage Causes in Safety Elements of Powered Roof Supports—A Case Study. *Energies* **2021**, *14*, 1027. [[CrossRef](#)]
5. Wojtecki, Ł.; Iwaszenko, S.; Apel, D.B.; Cichy, T. An Attempt to Use Machine Learning Algorithms to Estimate the Rockburst Hazard in Underground Excavations of Hard Coal Mine. *Energies* **2021**, *14*, 6928. [[CrossRef](#)]
6. Huang, X.; Liu, Q.S.; Qiao, Z. Research on Large Deformation Mechanism and Control Method of Deep Soft Roadway in Zhuji Coal Mine. *Rock Soil Mech.* **2012**, *33*, 827–834. [[CrossRef](#)]
7. Yu, Y.; Wang, X.Y.; Bai, J.B.; Zhang, L.Y.; Xia, H.C. Deformation Mechanism and Stability Control of Roadway Surrounding Rock with Compound Roof: Research and Applications. *Energies* **2020**, *13*, 1350. [[CrossRef](#)]
8. Wang, W.M.; Gao, X.; Jing, J.D.; Liu, C.L.; Zhou, J.H. Study on Roof Bolting with Anchor and Wire Mesh Coupling Support Technology in Weakly Consolidated Soft Rock Roadway. *Coal Sci. Technol.* **2014**, *42*, 23–26.
9. Hou, C.J.; Wang, X.Y.; Bai, J.B.; Meng, N.K.; Wu, W.D. Basic Theory and Technology Study of Stability Control for Surrounding Rock in Deep Roadway. *J. China Univ. Min. Technol.* **2021**, *50*, 1–12.
10. Stankus, J.C.; Peng, S.S. Floor Bolting for Control of Mine Floor Heave. *Int. J. Rock Mech. Min. Sci. Geomech. Abstr.* **1994**, *46*, 1099–1102.
11. Du, X.J.; Su, X.G.; Yuan, H.H.; Li, B.K.; Zhang, S.; Yang, Z.Y. Control of Surrounding Rock Stability Based on Failure Characteristics Analysis of Roadway Shoulders. *Saf. Coal Min.* **2015**, *46*, 62–65. [[CrossRef](#)]
12. Jiang, L.S.; Zhang, P.P.; Kong, P.; Jia, J.F.; Ma, N.; Shu, J.M.; Zhang, C. Rib-Control Support Principle Based on the Foundation Rigidity of Coal Mine Roadways. *J. China Coal Soc.* **2019**, *44*, 1020–1029. [[CrossRef](#)]
13. Yu, Y.; Lu, J.F.; Chen, D.C.; Pan, Y.X.; Zhao, X.Q.; Zhang, L.Y. Study on the Stability Principle of Mechanical Structure of Roadway with Composite Roof. *Minerals* **2021**, *11*, 1003. [[CrossRef](#)]
14. Wu, P.; Chen, L.; Li, M.; Wang, L.; Wang, X.F.; Zhang, W. Surrounding Rock Stability Control Technology of Roadway in Large Inclination Seam with Weak Structural Plane in Roof. *Minerals* **2021**, *11*, 881. [[CrossRef](#)]
15. Yang, R.S.; Li, Y.L.; Guo, D.M. Deformation and Failure Causes and Support Technology of Deep High Stress Soft Rock Roadway. *J. Min. Saf. Eng.* **2017**, *34*, 1035–1041.
16. Liu, Q.S.; Liu, X.W.; Huang, X.; Liu, B. Research on the Floor Heave Reasons and Supporting Measures of Deep Soft-Fractured Rock Roadway. *J. China Coal Soc.* **2013**, *38*, 566–572.
17. Ma, N.J.; Zhao, X.D.; Zhao, Z.Q.; Li, J.; Guo, X.F. Stability Analysis and Control of Roof in Deep Mining Roadway. *J. China Coal Soc.* **2015**, *40*, 2287–2295. [[CrossRef](#)]
18. Li, G.; Ma, F.; Guo, J.; Zhao, H.; Liu, G. Study on Deformation Failure Mechanism and Support Technology of Deep Soft Rock Roadway. *Eng. Geol.* **2019**, *264*, 105262. [[CrossRef](#)]
19. He, M.C.; Xie, H.P.; Peng, S.P.; Jiang, Y.D. Research on Mechanics of Rock Mass in Deep Mining. *Chin. J. Rock Mech Eng.* **2005**, *16*, 2803–2813.
20. Wang, R.C.; Tan, Y.L. Experimental study on failure mechanism of soft rock roadway in Yangcheng coal. *Appl. Mech. Mater.* **2014**, *675–677*, 1381–1384. [[CrossRef](#)]
21. Cheon, D.S.; Jeon, S.; Park, C.; Song, W.K.; Park, E.S. Characterization of Brittle Failure Using Physical Model Experiments under Polyaxial Stress Conditions. *Int. J. Rock Mech. Min. Sci.* **2011**, *48*, 152–160. [[CrossRef](#)]
22. Sun, L.H.; Yang, B.S.; Sun, C.D.; Li, X.; Wang, Z.W. Experimental Research on Mechanism and Controlling of Floor Heave in Deep Soft Rock Roadway. *J. Min. Saf. Eng.* **2017**, *34*, 236–242. [[CrossRef](#)]
23. Si, X.F.; Huang, L.Q.; Gong, F.Q.; Liu, X.L.; Li, X.B. Experimental Investigation on Influence of Loading Rate on Rockburst in Deep Circular Tunnel under True-Triaxial Stress Condition. *J. Cent. South Univ.* **2020**, *27*, 2914–2929. [[CrossRef](#)]
24. Zhao, X.Z.; Zhang, H.W.; Cao, C.; Zhang, M.; Zhang, H.D.; Han, J. Optimization of Bolt Rib Spacing and Anchoring Force under Different Conditions of Surrounding Rock. *Rock Soil Mech.* **2018**, *39*, 1263–1270, 1280. [[CrossRef](#)]
25. Yu, W.J.; Wu, G.S.; Liu, Z.; Huang, Z.; Liu, F.F.; Ren, H. Uniaxial Compression Test of Coal-Rock-Bolt Anchorage Body and Mechanical Mechanisms of Bolts. *Chin. J. Rock Mech. Eng.* **2020**, *39*, 57–68. [[CrossRef](#)]
26. Jing, H.W.; Yin, Q.; Zhu, D.; Sun, Y.J.; Wang, B. Experimental Study on the Whole Process of Instability and Failure of Anchorage Structure in Surrounding Rock of Deep-Buried Roadway. *J. China Coal Soc.* **2020**, *45*, 889–901. [[CrossRef](#)]
27. Li, B.; Gao, P.; Cao, Y.; Gong, W.; Zhang, S.; Zhang, J. Damage and Failure Characteristics of Surrounding Rock in Deep Circular Cavern under Cyclic Dynamic Load: A True Triaxial Experiment Investigation. *Minerals* **2022**, *12*, 134. [[CrossRef](#)]
28. Wu, G.H.; Yu, W.J.; Liu, Z.; Liu, F.F.; Huang, Z. Inversion Method of Mechanical Parameters of Rock Mass in Soft Rock Roadway and Its Engineering Application. *Ind. Min. Auto.* **2018**, *44*, 41–48. [[CrossRef](#)]
29. Wang, D.; Jiang, Y.J.; Sun, X.M.; Luan, H.J.; Zhang, H. Nonlinear Large Deformation Mechanism and Stability Control of Deep Soft Rock Roadway: A Case Study in China. *Sustainability* **2019**, *11*, 6243. [[CrossRef](#)]
30. Lecomte, A.; Salmon, R.; Yang, W.; Marshall, A.; Purvis, M.; Prusek, S.; Bock, S.; Gajda, L.; Dziura, J.; Niharra, A.M. Case Studies and Analysis of Mine Shafts Incidents in Europe. In Proceedings of the International Conference on Shaft Design and Construction, London, UK, 24–26 April 2012; Available online: <https://hal-ineris.archives-ouvertes.fr/ineris-00973661> (accessed on 1 April 2012).
31. Song, G.; Stankus, J.C. Control Mechanism of a Tensioned Bolt System in the Laminated Roof with a Large Horizontal Stress. In Proceedings of the 16th International Conference on Ground Control in Mining, Morgantown, WV, USA, 1 December 1996; pp. 167–172.

32. Kang, H. Support Technologies for Deep and Complex Roadways in Underground Coal Mines: A Review. *Int. J. Coal Sci. Technol.* **2014**, *1*, 261–277. [[CrossRef](#)]
33. Kwasniewski, J.; Dominik, I.; Lalik, K.; Sakeb, A.A. Analysis of Dependence between Stress Change and Resonance Frequency for Self-Excited Acoustical System. *Sol. State Pheno.* **2014**, *208*, 194–199. [[CrossRef](#)]
34. Skrzypkowski, K.; Korzeniowski, W.; Zagórska, A. Modified Rock Bolt Support for Mining Method with Controlled Roof Bending. *Energies* **2020**, *13*, 1868. [[CrossRef](#)]
35. Zhao, C.X.; Li, Y.M.; Liu, G.; Meng, X.R. Mechanism Analysis and Control Technology of Surrounding Rock Failure in Deep Soft Rock Roadway. *Eng. Fail. Ana.* **2020**, *115*, 104611. [[CrossRef](#)]
36. Malkowski, P. The Impact of the Physical Model Selection and Rock Mass Stratification on the Results of Numerical Calculations of the State of Rock Mass Deformation around the Roadways. *Tunn. Undergr. Space Technol.* **2015**, *50*, 365–375. [[CrossRef](#)]
37. Zhu, W.X.; Jing, H.W.; Yang, L.J.; Pan, B.; Su, H.J. Strength and Deformation Behaviors of Bedded Rock Mass under Bolt Reinforcement. *Int. J. Min. Sci. Technol.* **2018**, *28*, 593–599. [[CrossRef](#)]
38. Guo, X.; Zheng, X.; Li, P.; Lian, R.; Liu, C.; Shahani, N.M.; Wang, C.; Li, B.; Xu, W.; Lai, G. Full-Stress Anchoring Technology and Application of Bolts in the Coal Roadway. *Energies* **2021**, *14*, 7475. [[CrossRef](#)]
39. Tang, B.; Yeboah, M.; Cheng, H.; Tang, Y.Z.; Yao, Z.S.; Wang, C.B.; Rong, C.X.; Wang, Z.H.; Liu, Q.S. Numerical Study and Field Performance of Rockbolt Support Schemes in TBM-Excavated Coal Mine Roadways: A Case Study. *Tunn. Undergr. Space Technol.* **2021**, *115*, 104053. [[CrossRef](#)]
40. Zuo, J.P.; Sun, Y.J.; Wen, J.H.; Wu, G.S.; Yu, M.L. Full-Space Collaborative Control Technology and Its Application for Deeply Buried Roadways. *J. Tsinghua Univ.* **2021**, *25*, 853–862. [[CrossRef](#)]
41. Itasca Consulting Group Inc. Fast Lagrangian Analysis of Continua (FLAC). Available online: <https://www.itascacg.com/software/FLAC3D> (accessed on 10 December 2021).
42. Jiang, P.; Kang, H.; Wang, Z.; Liu, Q.; Yang, J.; Gao, F.; Wang, X.; Zhang, Q.; Zheng, Y.; Wang, H. Principle, Technology and Application of Soft Rock Roadway Strata Control by Means of “Rock Bolting, U-Shaped Yielding Steel Arches and Back Filling” in Synergy in 1000 M Deep Coal Mines. *J. China Coal Soc.* **2020**, *45*, 1020–1035. [[CrossRef](#)]
43. Fan, L.; Wang, W.; Yuan, C.; Peng, W. Research on Large Deformation Mechanism of Deep Roadway with Dynamic Pressure. *Energy Sci. Eng.* **2020**, *8*, 3348–3364. [[CrossRef](#)]
44. Kang, H. Sixty Years Development and Prospects of Rock Bolting Technology for Underground Coal Mine Roadways in China. *J. China Univ. Mining Technol.* **2016**, *45*, 1071–1081.
45. Wang, W.C.; Wang, Z.; Feng, Z.B.; Xu, Y.J. Research on Bolt-Mesh-Anchor Coupling Support Technology of Gateway with Deep Soft Rock Roadway. *Coal Technol.* **2019**, *38*, 8–11. [[CrossRef](#)]
46. Benmokrane, B.; Chennouf, A.; Mitri, H.S. Laboratory Evaluation of Cement-Based Grouts and Grouted Rock Anchors. *Int. J. Rock Mech. Min. Sci.* **1995**, *32*, 633–642. [[CrossRef](#)]
47. Zhou, W. *Advanced Rock Mechanics*; China Water and Power Press: Beijing, China, 1990.
48. Lu, Y.; Wang, L.; Zhang, B. An Experimental Study of a Yielding Support for Roadways Constructed in Deep Broken Soft Rock under High Stress. *Min. Sci. Technol.* **2011**, *21*, 839–844. [[CrossRef](#)]
49. Xie, Z.Z.; Zhang, N.; Han, C.L.; An, Y.P. Research on Principle and Application of Roof Thick Layer Cross-Boundary Anchorage in Coal Roadways. *Chin. J. Rock Mech. Eng.* **2021**, *40*, 1195–1208.
50. Zhang, K.; Zhang, G.; Hou, R. Stress Evolution in Roadway Rock Bolts during Mining in a Fully Mechanized Longwall Face, and an Evaluation of Rock Bolt Support Design. *Rock Mech. Rock Eng.* **2015**, *48*, 333–344. [[CrossRef](#)]
51. Gao, F.; Wang, X. Analysis on Sensitive Normal Test of Bolt Support Parameters for Mining Gateway. *Coal Sci. Technol.* **2007**, *11*, 68–72. [[CrossRef](#)]